Supplementary Material to *Paleoseismic history of faults ruptured in the 2019 Ridgecrest, California earthquake sequence* by Pierce et al.

Contents:

1. Detailed Luminescence Dating Methods

Sample preparation

Samples were prepared at the Desert Research Institute Luminescence Research Laboratory (Reno, Nevada). Potassium-rich feldspar grains were isolated from bulk sediment using standard preparation procedures (Aitken, 1998). Samples were treated with 10% HCl and 30% H_2O_2 to remove carbonates and organic matter and wet sieved to obtain the 180-250 µm grain size fraction. Heavy liquid separation using lithium heteropolytungstate (<2.58 g/cm^3) was used to isolate potassium feldspar grains. All samples except OV020 and OV021 were etched with 10% HF for 10 minutes to remove the outer alpha-irradiated layer.

Single-grain measurements were conducted using aluminum discs containing 100 holes (300 µm diameter and depth) arranged in a 10 x 10 grid.

Instrumentation

Luminescence measurements were performed on a Risø TL-DA-20 luminescence reader equipped with a focused infrared laser (830 nm; ~150 mW/cm^2) for single-grain stimulation and infrared LEDs (870 nm; ~115 mW/cm^2 at the sample position). Luminescence signals were detected through Corning/Kopp 7-59 and Schott BG39 filters transmitting wavelengths between 320-460 nm using a H7360-02 photomultiplier tube.

Measurement protocol

Equivalent dose (D_e) measurements were conducted using a modified single-aliquot regenerative dose (SAR) protocol (Murray and Wintle, 2000, 2003) applied to the IR_{50} signal (Wallinga, 2000). A preheat and cutheat of 160 °C and a hotwash of 180 °C were used.

A dose recovery test was conducted on 600 grains from sample OV001. Grains were first bleached using IR LEDs for 1000 seconds and then given a laboratory beta dose of 22 Gy. The measured-to-given dose ratio was 0.95 ± 0.01.

Dose response curves were fit with an exponential function.

Grain rejection criteria

Grains were excluded if they exhibited:

- test dose uncertainty >10%

- recycling ratio error >10%
- recuperation >5%
- luminescence signals <3σ above background

All individual D_e values include a 2.5% instrumental uncertainty.

Zero-dose grains (negative D_e values or values consistent with zero within uncertainty) and saturated grains ($D_e > 2D_0$ or grains that did not intersect the dose-response curve) were excluded following Wintle and Murray (2006).

Statistical modeling

Equivalent dose distributions displayed moderate overdispersion (>40%). Most samples exhibited symmetrical distributions and were modeled using the Central Age Model (CAM; Galbraith et al., 1999). Samples OV001, OV028, and OV029 displayed evidence of post-depositional mixing characterized by populations of low-dose grains and elevated overdispersion; these samples were analyzed using the Finite Mixture Model (FMM; Galbraith and Green, 1990).

Fading measurements

Anomalous fading rates (g-values) were measured following the method of Auclair et al. (2003) after D_e measurements. Reported g-values represent weighted means of measurements made on single-grain discs (100 grains per disc).

Dose rate and age calculation

Radioelement concentrations (U, Th, and K) were measured using ICP-MS and ICP-AES at ALS Geochemistry. Gravimetric moisture content ranged from 1-2% and was used to correct dose rates while including a 5% uncertainty to account for long-term moisture variability.

Dose rate and age calculations follow Durcan et al. (2015). Final luminescence ages were corrected for anomalous fading using the model of Huntley and Lamothe (2001).

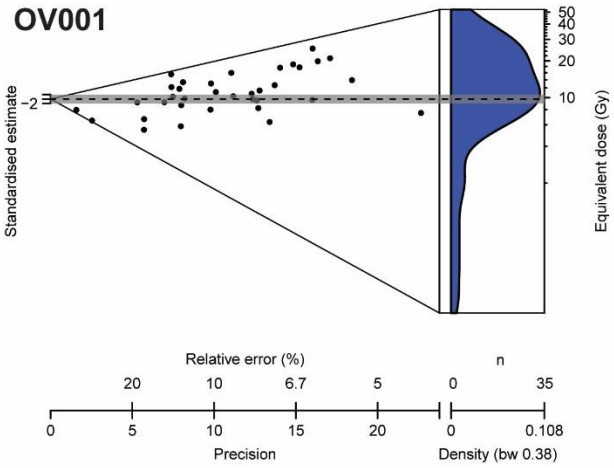
OV001
Standardised estimate
Equivalent dose (Gy)
Relative error (%)
n
Precision
Density (bw 0.38)

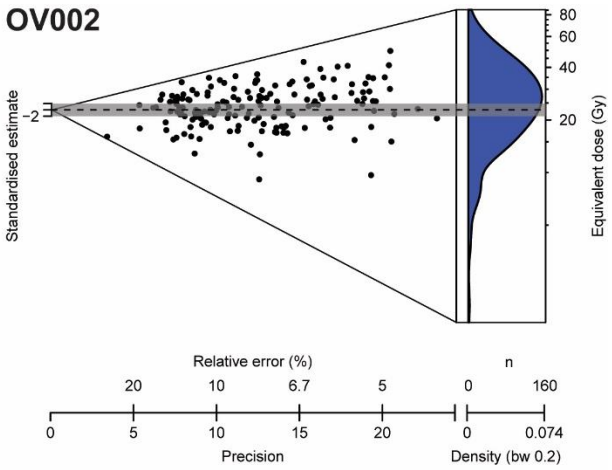
OV002
Standardised estimate
Equivalent dose (Gy)
Relative error (%)
n
Precision
Density (bw 0.2)

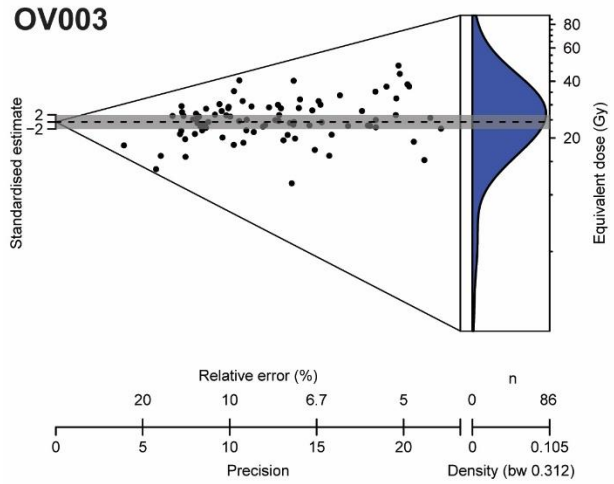
OV003
Standardised estimate
Equivalent dose (Gy)
Relative error (%)
n
Precision
Density (bw 0.312)

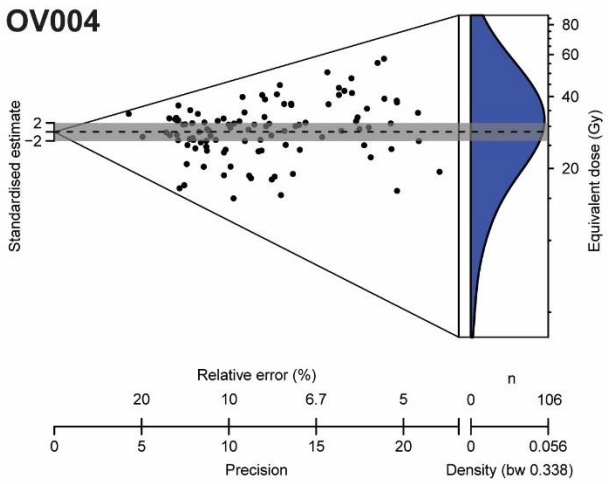
OV004
Standardised estimate
Equivalent dose (Gy)
Relative error (%)
n
Precision
Density (bw 0.338)

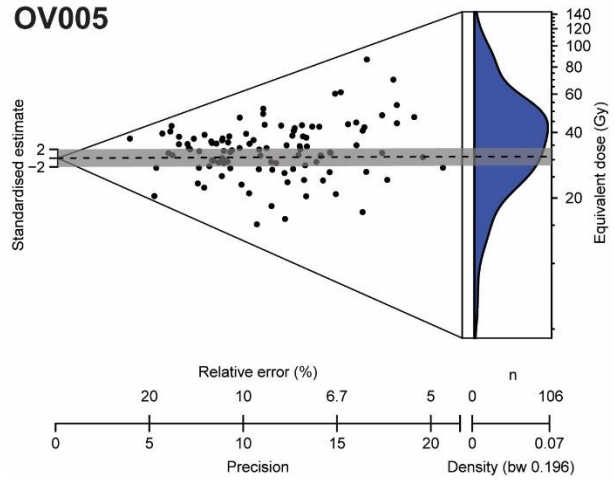
OV005
Standardised estimate
Equivalent dose (Gy)
Relative error (%)
n
Precision
Density (bw 0.196)

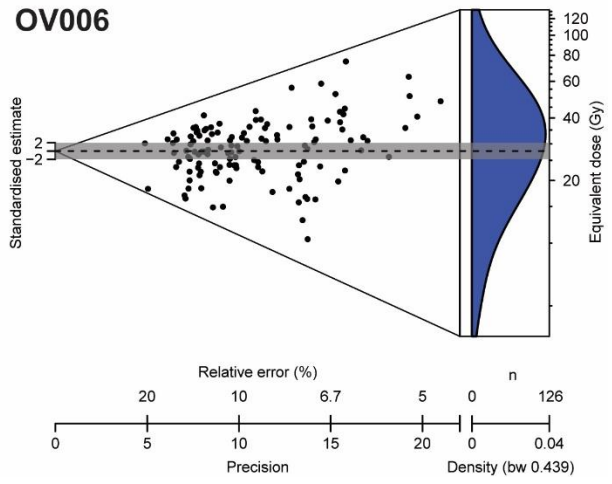
OV006
Standardised estimate
Equivalent dose (Gy)
Relative error (%)
n
Precision
Density (bw 0.439)

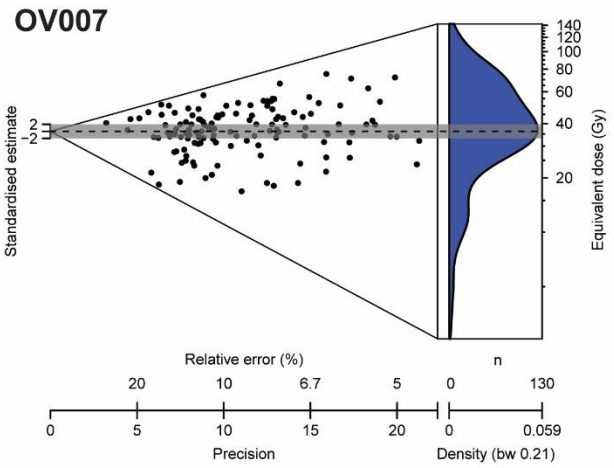
OV007
Standardised estimate
Equivalent dose (Gy)
Relative error (%)
n
Precision
Density (bw 0.21)

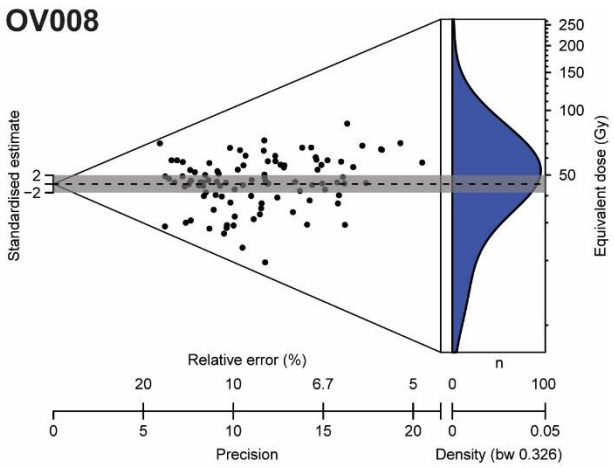
OV008
Standardised estimate
Equivalent dose (Gy)
Relative error (%)
n
Precision
Density (bw 0.326)

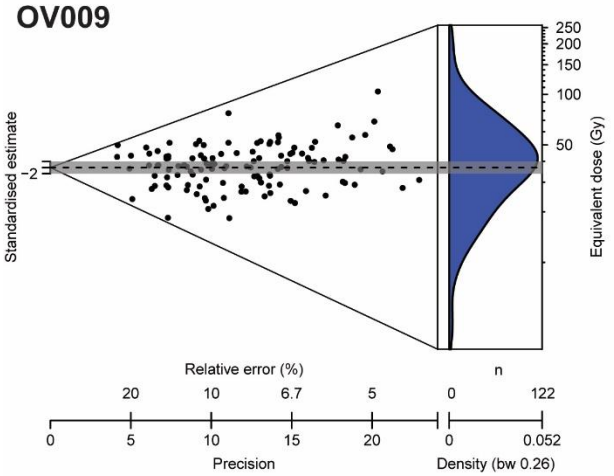
OV009
Standardised estimate
Equivalent dose (Gy)
Relative error (%)
n
Precision
Density (bw 0.26)

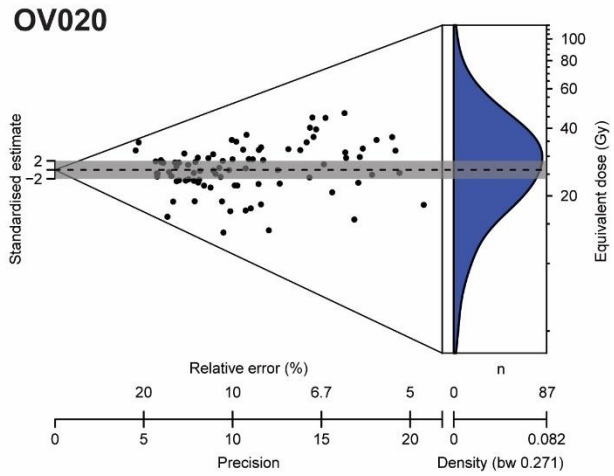
OV020
Standardised estimate
Equivalent dose (Gy)
Relative error (%)
n
Precision
Density (bw 0.271)

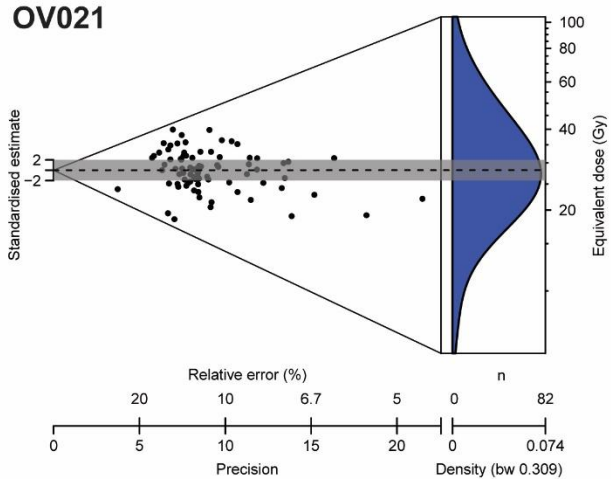
OV021
Standardised estimate
Equivalent dose (Gy)
Relative error (%)
n
Precision
Density (bw 0.309)

2. Trench logs not shown in text

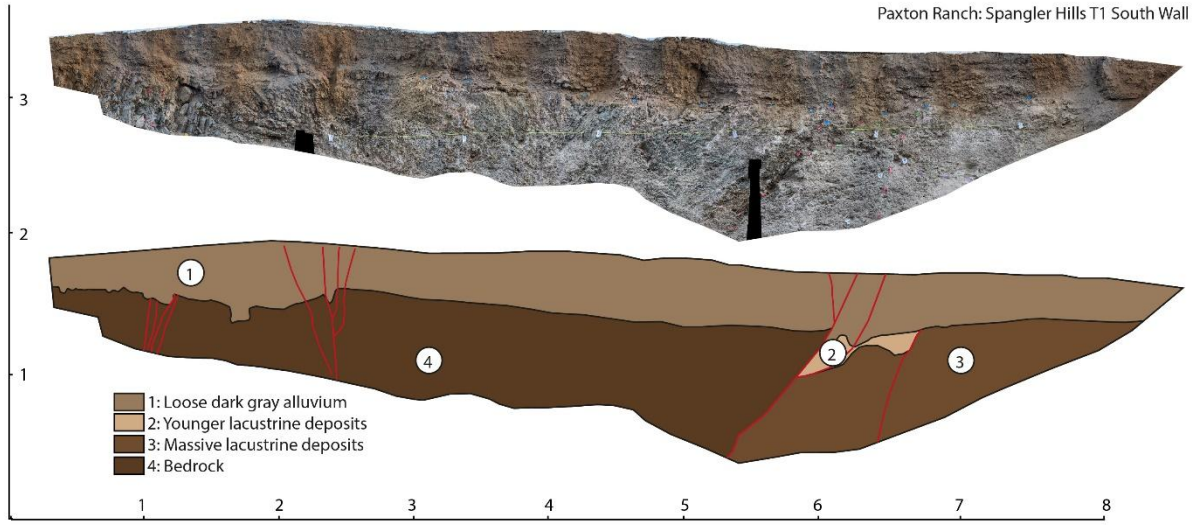

SH-T1: Thin Holocene stratigraphy precluded discerning individual events, and two primary shear zones are present here both rupturing in the 2019 M7.1 earthquake.

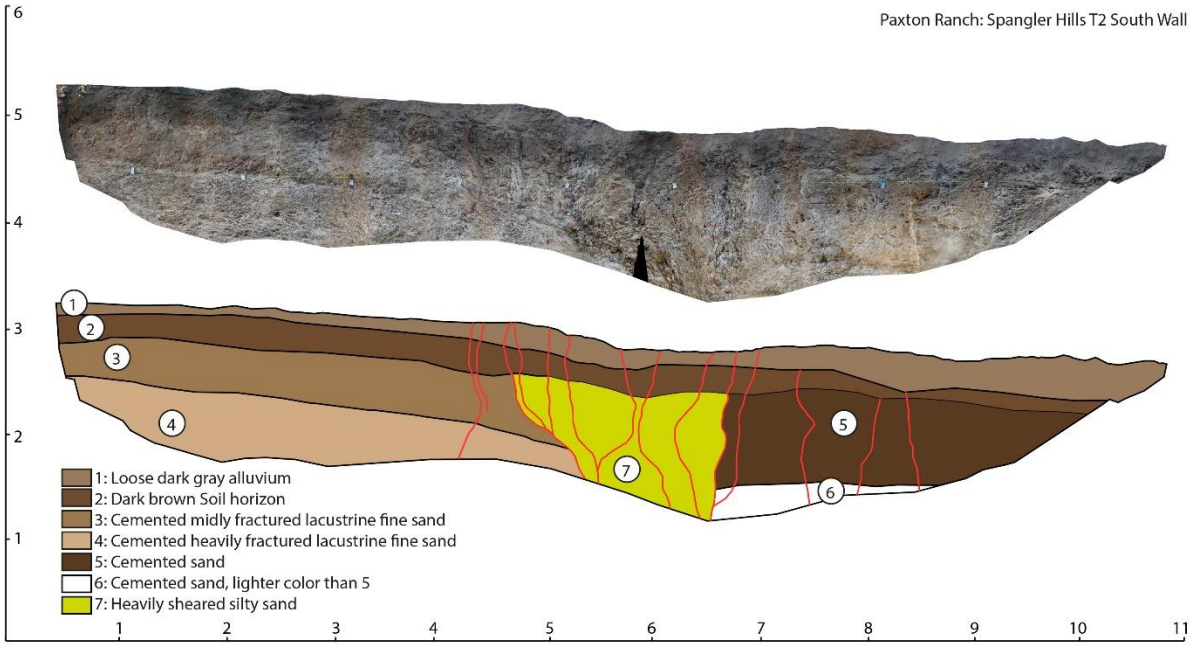

SH-T2: Thin Holocene stratigraphy precluded discerning younger events. A wide heavily sheared zone provides evidence of multiple late Quaternary events.